Optimization MRI Cylindrical Coils Using Discretized Stream Function With High Order Smoothness

Zhenyu Liu[1], Feng Jia[2], Jürgen Hennig[3], and Jan G. Korvink[2,4]

[1]State Key Laboratory of Applied Optics, Changchun Institute of Optics, Fine Mechanics and Physics (CIOMP), Chinese Academy of Sciences, 130033 Changchun, China
[2]Freiburg Institute of Advanced Studies (FRIAS), University of Freiburg, 79110 Freiburg, Germany
[3]Department of Radiology, Medical Physics, University Hospital Freiburg, 79110 Freiburg, Germany
[4]Department of Microsystems Engineering (IMTEK), University of Freiburg, 79110 Freiburg, Germany

The design of coil for magnetic resonance image (MRI) application is an optimization problem, in which a specified distribution of the magnetic field inside a region of interest is generated by choosing the optimal distribution of current density on a specified non-intersecting design surface. This paper proposes an iterative optimization method for designing MRI coils on a cylindrical surface by using a piecewise discretized scalar stream function as design variable. The surface current density is accurately calculated using piecewise interpolation with C^1 smoothness based on the developable property for a cylindrical surface. MRI coils are designed by choosing bi-objective functions and pseudo-Newton sensitivity analysis. The smoothness of the coil are maintained by adjusting the value of derivative degrees of freedom of design variables which are used to interpolate the stream function. Pareto points provide more flexible choices between the two complementary objectives.*

***Index Terms*—C^1 smoothness, developable surface, MRI coil.**

I. Introduction

MAGNETIC RESONANCE IMAGING (MRI) is a widely used technique in radiology to visualize the structure and function of the body. It can provide detailed images of the body in any section plane, and has good contrast between the different soft tissues of the body. This makes the MRI technique especially useful in neurological, cardiovascular, and oncological imaging. In an MRI scanner there are three main parts, a main magnet, the gradient coils, and radio frequency transmitters and receivers. The main magnet is the largest component of the scanner used to generate a static and homogeneous magnetic field $\vec{B}_0$. The remainder of the scanner is built around it. Gradient coils spatially encode the positions of protons by varying the magnetic field across the imaging volume. The radio frequency transmission system consists of a RF synthesizer, a power amplifier and a transmitting coil. The radio frequency receiver consists of coils, a pre-amplifier and a signal processing system. In this paper, a method for the design of an MRI coil which can generate a specified distribution of magnetic field is discussed.

The design of MRI coils is an *optimization problem*. For a magnetostatic calculation, if all the electric currents $\vec{J}$ in a system are known, then the magnetic field $\vec{B}$ can be determined by the *Biot-Savart* method. This is called the *forward problem*. If a spatial distribution of the magnetic field inside a *region of interest* (ROI) Ω_{ROI} is specified, and the goal is to find the optimal distribution of the electric current density $\vec{J}$ on a specified design surface Γ_{coil}, this is called the *optimization problem*. Over the past 20 years many papers have discussed theoretical methodologies for designing MRI coils. A typical design procedure mainly includes two steps, one to calculate the spatial distribution of the magnetic field inside a ROI, the other to search for the optimal distribution of the electric current density on a specified design surface. Among the methods which have been proposed to design MRI coils, the target field method is the most widely used one [1], [2]. In the target field method, the magnetic field $\vec{B}$ is usually calculated using the *Biot-Savart* method or the series expansion method where the design surface belongs to regular surfaces, such as planar and cylinder surfaces. The target value of magnetic field distribution is used through the collocation method in order to interpolate a coefficients matrix for an analytical expression of the target magnetic field. The optimal distribution of the electric current density is solved using the inverse of the coefficient matrix and the value of magnetic field at the collocation points. Because of the analytical nature of the target field method, in principle a linear algebra equation needs to be solved once. Currently, the original target field method has developed as a mature procedure to design a couple of MRI coils, where merely part of these progresses are listed here as the finite length coil, the multiple layer coils which has shimming or self-shielding function, the coil which has minimized value of inductance or resistance, the coil with balanced torque and other physical quantities [3]–[17].

Even though the target field method has obtained a big success for designing MRI coils, the essence of design methodology still faces a challenge that the design surface should be regular one. In order to extend the usage of MRI coils, one requires a design method which can flexible express the electric current density on a general design surface. Recently, the stream function method has been used to design MRI coils on more

Manuscript received April 08, 2010; revised August 03, 2011; accepted September 30, 2011. Date of publication October 13, 2011; date of current version March 02, 2012. Corresponding author: Z. Liu (e-mail: liuzy@ciomp.ac.cn).

Color versions of one or more of the figures in this paper are available online at http://ieeexplore.ieee.org.

*Part of this work has been published in conference ISMRM 2009

Digital Object Identifier 10.1109/TMAG.2011.2171355

general design surfaces [18]–[23]. If a design surface Γ_{coil} is simply connected, or if every closed curve in Γ_{coil} can be shrunk to a point in a continuous way, it is known that there is a scalar function ψ such that a surface current density can be directly expressed as

$$\vec{J} = \nabla \times (\psi \cdot \vec{n}) \tag{1}$$

where $\vec{n}$ is the normal vector of the current sheet Γ_{coil}, and the surface current density $\vec{J}$ satisfies the divergence-free condition $\nabla \cdot \vec{J} = 0$. The scalar function ψ is known as the stream function [24]. When the stream function is expressed using a combination of discretized meshes, such as the mesh used in the finite element method or the boundary element method, a design surface can be extended to piecewise smoothed surfaces with arbitrary shape of boundary, and the value of the magnetic field $\vec{B}$ can be calculated by using the numerical integration of the *Biot-Savart* method. The accuracy of the value $\vec{B}$ directly depends on the accuracy of $\vec{J}$ and the numerical integration method. For the case that the design surface Γ_{coil} is piecewise smoothed, the accuracy of the numerical integration can be maintained by choosing a list of suitable integration points [25]. Therefore, the calculation of the surface current density is a key point to maintain the quality of the designed coils.

Physically, a surface current density $\vec{J}$ is continuous inside a design surface Γ_{coil}. Based on (1), this implies that $\nabla\psi$ and $\vec{n}$ should be both continuous inside a Γ_{coil}. There are a couple of ways to calculate the surface current density on a curved surface, especially for a cylindrical surface. For example, cylindrical coordinate instead of Cartesian coordinate can be chosen to express a point on cylindrical surface directly [26]. A piecewise three-dimensional element with curved-edge [27], [28] or a planar element [22], [23] can be used to discretized cylindrical surface. It is an active and challenging research topic to construct a three dimensional curved-edge element. For a planar element discretization, the discretization error could be reduced by using a mesh refinement method. However, one has to balance the computational accuracy with the resulting computational cost. In order to accurately express a physically continuous current density $\vec{J}$ on a cylindrical surface, a discretization of the scalar stream function with high order smoothness on a developed cylindrical surface is proposed in this paper. The cylinder is a typical developable surface and also the most widely used design surface for MRI coils. The authors are of the opinion that many other alternative methods are available to design MRI coils on cylindrical surface by using discretized stream function design variables. The design method proposed in this paper is the one which is mainly focus on a theoretical point of view that developable surface can be an alternative way to implement a true continuous current density expression in the stream function method. When combined with the high-order numerical integration method, a high accuracy result can be obtained to design MRI coils on a full or cut cylindrical surfaces.

II. Numerical Solution of Magnetostatics in Cylindrical Coordinate

A cylindrical surface is a developable surface which has zero Gaussian curvature everywhere [29]. It has the property that it can be extended into a two dimensional sheet. One can express a cylindrical surface using cylindrical coordinates (r_0, θ, z). For a cylindrical surface, the parameter r_0 has a fixed value. The surface current density $\vec{J}$ in (1) is expressed as

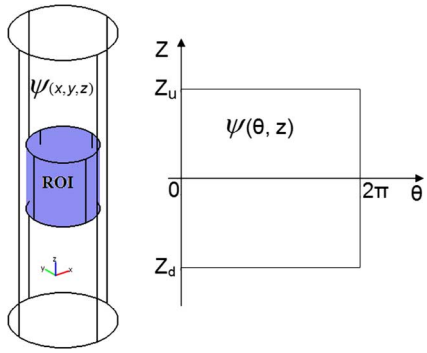

Fig. 1. Current-carrying surface Γ_{coil}, region of interest (ROI), and the developed design surface.

$$\nabla \times (\psi \cdot \vec{n}) = (0, \frac{\partial \psi}{\partial z}, -\frac{1}{r_0}\frac{\partial \psi}{\partial \theta})^T \tag{2}$$

where $\vec{n} = (1, 0, 0)^T$ in cylindrical coordinates. The x and y components of the surface current density are

$$\begin{aligned} J_x(\theta, z) &= -\frac{\partial \psi(\theta, z)}{\partial z} sin(\theta) \\ J_y(\theta, z) &= \frac{\partial \psi(\theta, z)}{\partial z} cos(\theta). \end{aligned} \tag{3}$$

The magnetic field B_z for a point (r_i, θ_i, z_i) inside a ROI is calculated using the Biot-Savart method in cylindrical coordinates as [26]

$$B_z(r_i, \theta_i, z_i) = \frac{\mu_0}{4\pi} \int_{z_l}^{z_u} \int_{0}^{2\pi} \frac{J_y(\theta, z) RC - J_x(\theta, z) RS}{(RC^2 + RS^2 + (z - z_i)^2)^{\frac{3}{2}}} r_0 d\theta dz \tag{4}$$

where

$$\begin{aligned} RC &= (r_0 cos\theta - r_i cos\theta_i) \\ RS &= (r_0 sin\theta - r_i sin\theta_i) \end{aligned} \tag{5}$$

r_0 is the radius of the current-carrying surface $[0, 2\pi] \times [z_l, z_u]$, and z_l and z_u are the lower and upper bounds of the cylindrical surface along the z direction (Fig. 1).

III. Interpolation of Stream Function Using Argyris Element

In order to express a physically continuous electric current density $\vec{J}$ in (1), the presence of a continuous first derivative is necessary for the steam function ψ. When using piecewise connected element to discretize a design surface Γ_{coil}, the design variable ψ is interpolated separately in each element. Typically a Lagrange element which uses the nodal value of the stream function as *degree of freedom* (DOF), is used to interpolate the distribution of a stream function in order to design MRI coils [30]–[32]. The advantage of a Lagrange element is that there is only one DOF on each node. When a high-order Lagrange element which has DOF on the element edge or

inside of element, the smoothness of the stream function can be improved inside an element but not on the edge between two neighbor elements. This is a characteristic for the element with C^0 continuity. When a Hermite type element with nodal derivative DOF is used, the continuity is recovered both inside the element and along the edge of the element. In order to obtain a C^1 continuity for the value of the stream function, one must have both the ψ, its tangential and normal derivatives $\partial\psi/\partial t$, $\partial\psi/\partial n$ which are uniquely defined inside each element. For a planar triangular element, the nodal DOFs should include $\psi, \partial\psi/\partial x, \partial\psi/\partial y, \partial^2\psi/\partial x^2, \partial^2\psi/\partial x\partial y, \partial^2\psi/\partial y^2$, and three normal slopes $\partial\psi/\partial n$ at the middle of each edge. Therefore, the total number of DOFs for a triangular element is 21. The interpolation function of the above element can be constructed with a complete quintic polynomial. This element was described by Argyris *et al.* in 1968 and is now named *Argyris* element [33], [34]. Because using triangular element is easier than quadrilateral elements to discretize a two-dimensional surface with arbitrary topology and shape, the *Argyris* triangle element is used in this paper to piecewise interpolate a stream function.

IV. Sensitivity Analysis

A commonly used optimization objective for designing MRI coil has the least square format

$$\text{Min}: \quad F = \int_{\Omega_{\text{ROI}}} (B_z - B_z^*)^2 \, d\Omega_{\text{ROI}} \tag{6}$$

where B_z^* is the z-component of the target magnetic field. In this paper, the numerical discretization method is used to calculate the magnetic field $\vec{B}$ at sampling points inside a ROI, therefore a discretized expression of (6) is

$$\text{Min}: \quad F = \sum_{i=1}^{k} \frac{\beta_i}{2} (B_{zi} - B_{zi}^*)^2 \tag{7}$$

where β_i is the weight coefficient for each discretized sampling point (r_i, θ_i, z_i), and k is the number of the sampling points inside the ROI. An optimization procedure includes several key steps which are run sequentially (Fig. 2). Among these, the most important steps are solving the magnetostatic problem and performing sensitivity analysis. For the step of solving the magnetostatic problem, a design surface with current distribution is discretized using a triangular elements on a developed cylindrical plane, and the value of a stream function is interpolated using

$$\psi = \sum_{j=1}^{nd} \alpha_j N_j \tag{8}$$

where N_j is the shape function of the $Argyris$ element, and nd is the number of DOFs which is used to interpolate ψ on the design surface Γ_{coil}. Using this high-order smooth interpolation strategy, the magnetic field B_z can be calculated accurately. In this paper, the sensitivity vector is obtained using a first-order derivative of the objective function. The simplest sensitivity analysis method is the *steepest descent* (SD) method in which the first-order derivative of the objective function is used directly with an adaptive step size searching algorithm. For the objective function (7), the first-order derivative is

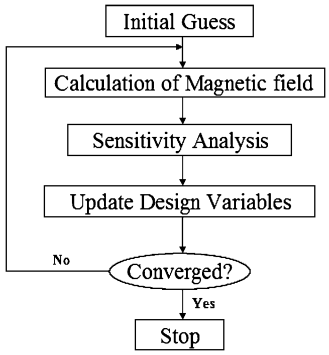

Fig. 2. Flowchart of a standard optimization procedure.

$$\frac{\partial F}{\partial \alpha_j} = \sum_{i=1}^{k} \beta_i (B_{zi} - B_{zi}^*) \frac{\partial B_{zi}}{\partial \alpha_j} \tag{9}$$

where

$$\frac{\partial B_{zi}}{\partial \alpha_j} = \frac{\mu_0}{4\pi} \int_{z_l}^{z_u} \int_{0}^{2\pi} \frac{\frac{\partial N_j}{\partial z}(cos\theta RC + sin\theta RS)}{(RC^2 + RS^2 + (z - z_i)^2)^{3/2}} r_0 d\theta dz. \tag{10}$$

Despite its simplicity, the performance of this method is limited by the smoothness of the objective function. At the same time, the convergence rate is very low in the proximity the optimal point. Another widely used method is the *conjugate gradient* (CG) method which avoids drawbacks of the SD method [35]. For a least-square type objective, one observes that the CG method is more efficient than the SD method. However, the numerical stability of the CG method is not as good as for the SD method. In principle, both the SD and CG methods are first-order methods. With an initial guess far away from the optimal point, the first-order method is found to have more stable performance than the Newton type method which needs second-order derivative data. Super-linear convergence of the Newton method will occur when the iteration gets sufficiently close to the optimal point. This property makes the Newton method more attractive than a first-order method. For a large-scale optimization problem, the biggest challenge associated with the Newton method is that the Hessian matrix is computationally very expensive to update, or even not available for certain objective functions. Therefore, many pseudo-Newton methods have been proposed. The *limited memory BFGS* (L-BFGS) method is such a method that avoids using the Hessian matrix [36]. In this paper, all three methods are used to demonstrate the performance for MRI coils optimization.

V. Numerical Implementation of Coil Design

In order to design MRI coils using the method proposed above, three issues need to be addressed.

A. Smoothing Stream Function

MRI coil design is an optimization problem. It is seldom that a design of MRI coil can be done without using any extra treatment [38]. When the stream function is used as the design vari-

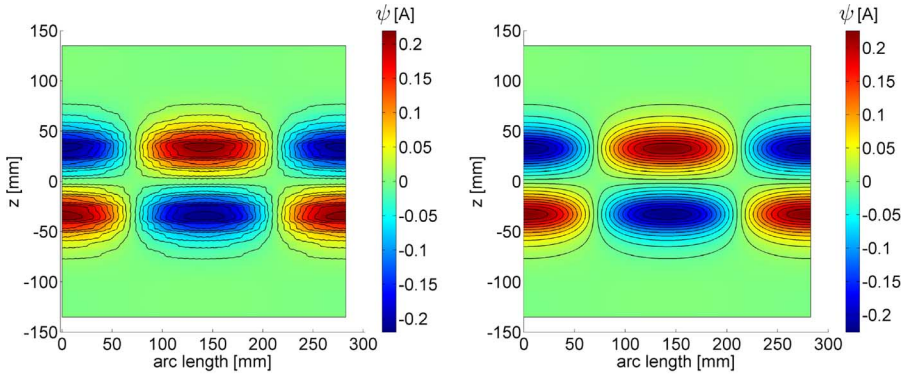

Fig. 3. Smoothing effect using the biharmonic equation. (a) Contours of stream function before smoothing. (b) Contours of stream function after smoothing.

able, the layout of the optimal coil is constructed based on the contour lines of the stream function surface. One typical phenomenon of the constructed coils is that the contour line of the stream function oscillates. There are two strategies which have been widely used to avoid the oscillation of the stream function. One strategy is the regularization method that a weighted regularization term is added to the optimization objective. The most commonly used regularization is the Tikhonov method

$$\text{Min}: \quad F = \int_{\Omega_{\text{ROI}}} (B_z - B_z^*)^2 \, d\Omega_{\text{ROI}} + \int_{\Gamma_{\text{coil}}} \lambda \psi^2 \, d\Gamma. \quad (11)$$

The key point of the Tikhonov regularization is to find a reasonably small positive value of λ so that the optimal solution of (11) is stable and close enough to the original objective function [39], [40]. The optimal regularization parameter λ is usually unknown for practical problems, and the magnitude of the optimal value of λ needs to be tuned based on certain algorithm [41]. There are a couple of choices for the regularization term which have been used to design MRI coils [9], [14], [42]. All of these method need to choose a suitable value of the weight parameter λ. The other strategy is the filter method which has been widely used for structural optimization [43]. Instead of adding additional regularization term into the original objective, filtering for the sensitivity vector or the stream function is implemented during an iterative loop. A unified expression of the filter technique is a pseudo time-dependent nonlinear diffusion equation [44]

$$\frac{d\psi}{dt} = \nabla \cdot (G(\psi) \nabla \psi) \quad (12)$$

where $G(\psi)$ is a nonlinear function used to control anisotropic diffusion, and the pseudo time t is used to control the range of diffusion effect. In fact, the pseudo time has a similar effect as the weight parameter λ in the regularization method. The longer pseudo time runs, the more smooth the stream function is. An over-used smoothing procedure by either choosing a large value of the weight parameter λ or a longer pseudo time interval, may excessively flatten the stream surface and slow down the optimization procedure. In this paper, a biharmonic equation is used to avoid numerical oscillations of the stream function. In principle, this method belongs to the filter strategy. Even though a similar smoothing effect can be alternative implemented by using a regularization method, the procedure used in this paper can avoid over smooth effect by explicitly limit the value of the stream function on mesh nodes. The biharmonic equation is a fourth-order *partial differential equation* (PDE) which arises in many areas of continuum mechanics [34]

$$\nabla^2 \nabla^2 \psi = 0. \quad (13)$$

Because the *Argyris* element is used to interpolate the stream function, all of the spatial derivative DOFs of the Argyris element can be adjusted simultaneously by solving (13) with nodal value of the stream function setting as the Dirichlet type point conditions. The above smoothing procedure can be explained as that the developed design surface is a thin plate and the nodal value of the stream function is the unchanged deformation of the plate, then the solution of stream function should have C^1 smoothness everywhere based on the characteristics of a fourth-order PDE. It is not necessary to choose a filter function $G(x)$ or a pseudo-time interval. The size of the mesh which used to discretize the design domain automatically adjusts the smoothing effect. Fig. 3 shows the smoothing effect of the biharmonic equation for an iterative step in designing the gradient coil with linear gradient of the magnetic field. The numerical solution of (13) is implemented using the commercial finite element software Comsol [45].

B. Open vs. Closed Coil

Usually, a closed coil with limited length is preferred to a coil with an open section. An opened coil may cause fabrication problems because it requires a round-back conductor which should be far away from the main part of a coil. Therefore, a design constraint needs to be added in order to limit the layout of the coil directly. Considering the discretization methodology used in this paper, a closed coil implies that the stream function has the same value on boundaries of the design surface. For the optimization model in (7), the surface current will not automatically flow along the boundary. The strategy used in this paper is as follows:

1) Mesh a design surface so that the boundary or any predefined closed curves coincide with the edges of the discretized elements.
2) Specify a zero initial value for the entire design surface.

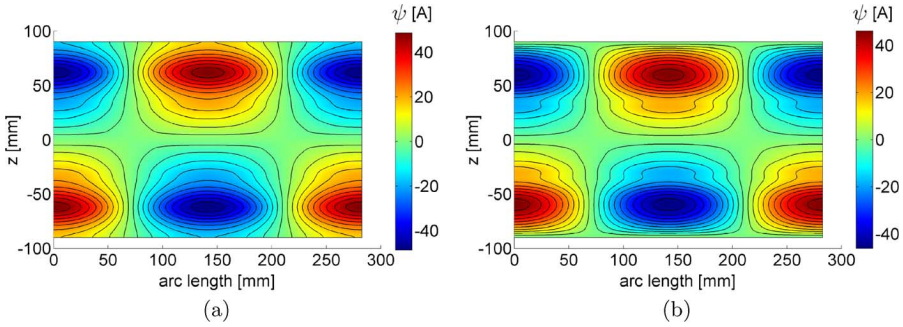

Fig. 4. Coil optimization with and without closed coil constraint. (a) Contours of stream function for open coils. (b) Contours of stream function for closed coils.

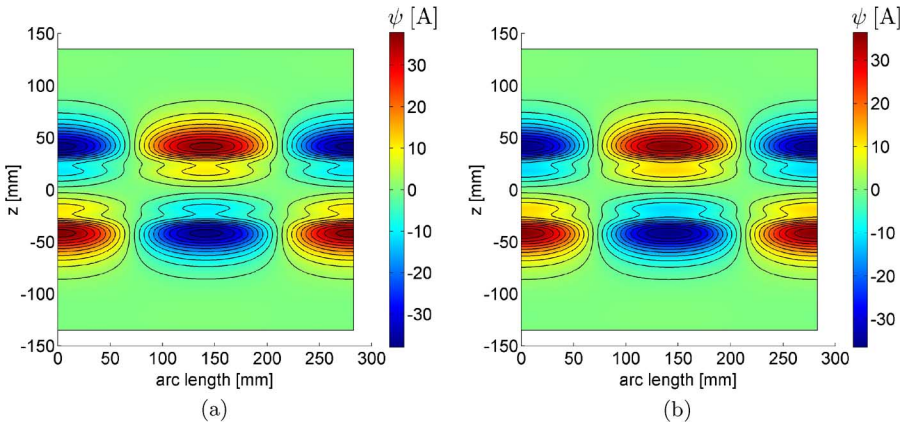

Fig. 5. Optimization of coil with and without symmetric constraint. (a) Contours of stream function without symmetric constraint. (b) Contours of stream function with symmetric constraint.

3) Specify the value of sensitivity on boundary points with the same value. This could be implemented using the average value of all the sensitivity on boundary points in which coil needs to be closed.

Using the above procedure, the value of the stream function is maintained as constant in each iteration, and may change its value simultaneously during the optimization procedure. Fig. 4 shows an example for open and closed coils, respectively.

C. Maintain Coil Symmetry

For a given optimization objective, the optimal layout of MRI coils may contain symmetries. A design surface can be chosen as a subset of the Γ_{coil} based on symmetrical property. However, the symmetry may differ among coils. Instead of choosing part of Γ_{coil} as the design surface, the whole cylinder surface is used as the design surface for all the numerical examples presented in this paper. The symmetry is maintained by adding additional constraints for the original sensitivity vector in (9). Even though this method is computationally more expensive than when only part of the Γ_{coil} is chosen as the design surface, the gain one obtains is that the optimization code can be extended to more general coil designs by only changing the expression of the optimization objective and the symmetry constraint for the original sensitivity vector. The component of the sensitivity in (10) will remain unchanged for an objective which relates to the magnetic field B_z directly. Therefore, it needs to be calculated once and the optimization can be run quite efficiently.

VI. MRI Coils Design on Cylindrical Surfaces

Gradient and shimming coils are two kinds of important coils in MRI. A gradient coil is used to generate a controllable magnetic gradients inside a ROI. A shimming coil is used to maintain the homogeneity of the main magnetic field $\vec{B}_0$. In this section, the design procedure for gradient coils and shimming coils are presented in order to illustrate the effect of the design method proposed in this paper. The computational domains in the Cartesian and developed cylindrical coordinates are shown in Fig. 6. The radius and height of the cylindrical coordinate surface is 45 mm and 270 mm respectively. The ROI has a cylindrical shape with radius and height 30 mm and 60 mm respectively. The ROI is discretized using a relatively regular mesh with 2301 nodal points, and the design surface Γ_{coil} is discretized with 2880 triangular elements. For the optimization objective (7), the weight β_i is set as 1 for all the sampling points inside the ROI. There are two stop criteria in this paper. The first stop criterion is a set of three different conditions which are expressed in the following formula [37]:

$$|F_k - F_{k-1}| < \epsilon(1 + |F_k|) \tag{14}$$

$$||\psi_k - \psi_{k-1}|| < \sqrt{\epsilon}(1 + ||\psi_k||) \tag{15}$$

$$||g_k|| < \sqrt[3]{\epsilon}(1 + |F_k|)\,. \tag{16}$$

Here, F_k, ψ_k and g_k are values of objective function, stream function and $\partial F/\partial\psi$ in (7)–(9) at the kth optimization step respectively. Users can control the desired accuracy by specifying the tolerance parameter ϵ which is set as 10^{-9} in this paper. The

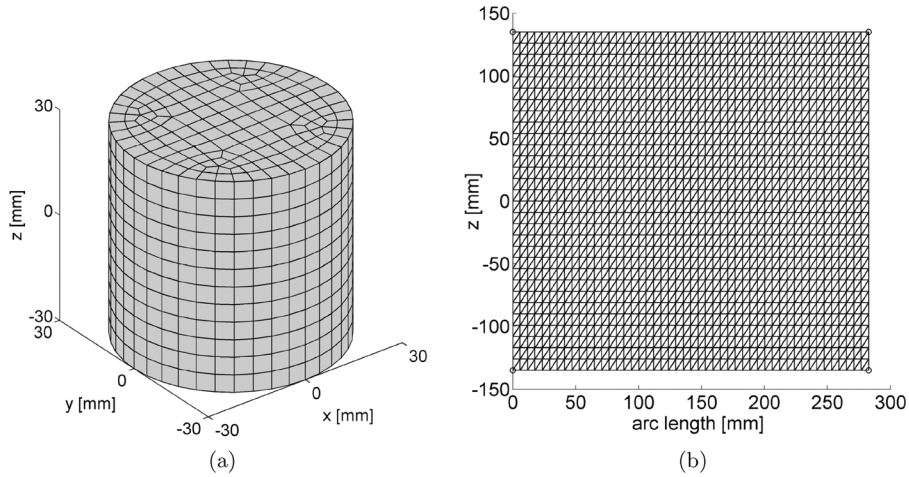

Fig. 6. Meshes in the region of interest (ROI) and on the developed design surface. (a) Mesh for the ROI. (b) Mesh for the design surface.

conditions (14) and (15) are employed to check whether the objective function and design variable converge respectively. At the same time, the necessary first order optimization condition is considered in the third condition (16). The second stop criterion is the *total number of objective function evaluations* (TNOFE) which is set as 500. Using this stop criterion, we can avoid unlimited loop and quantify computational resources in the optimization procedure. Fig. 8 shows the convergent history for the design of cylindrical gradient coil which can generate a linear changed magnetic field along the x axis inside the ROI. The target gradient strength in the center of the ROI is 10 mT/m. The stream function and coil layout (the contour lines of the stream function) are shown in Fig. 7. Here, another residual $\triangle G_x$ is used to denote the linear gradient deviation of magnetic field:

$$\triangle G_x = \left| \frac{\partial B_z/\partial x - \partial B_z^*/\partial x}{\partial B_z^*/\partial x} \right|. \tag{17}$$

Generally, in order to satisfy the requirement in the MRI engineering, the maximum of $\triangle G_x$ is less than 5%. It shows that the L-BFGS has much better performance than the SD and CG method. For the L-BFGS, an initial approximate Hessian is equal to a unit diagonal matrix. Users need to choose a non-negative integral M so that the stored sensitivity during the previous M iterations are used to construct the current sensitivity vector. Note that the Hessian matrix of the L-BFGS is equivalent to the BFGS Hessian matrix if $M = \infty$ which is not a realistic option in practice. Normally, the convergence rate of the L-BFGS depends on the value of M [36]. Table I shows the performance of the L-BFGS when designing the above gradient coil. It shows that the number of iterations used for the whole optimization procedure will decrease when choosing a relatively large value of M. However, too large a value of M will not lead to a better performance, especially in terms of storage requirements and computational cost.

Compared with the gradient coil design, the difference for the shimming coil design is to modify the expression of B_z^* in (7), and to specify a symmetrical constraint for the original sensitivity vector. For an iterative optimization procedure, the sensitivity analysis is often the most time-consuming step. When

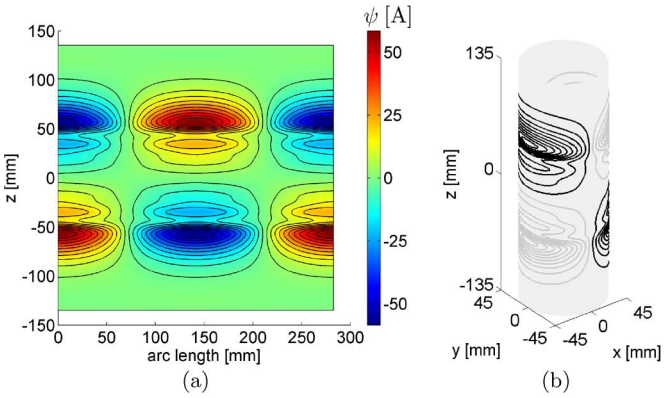

Fig. 7. Stream function contours and its corresponding layout of gradient coil for target magnetic field gradient 10 mT/m. (a) Stream function and its contours using L-BFGS with $\mathrm{M} = 9$. (b) Layout of gradient coil with current 5.8528A.

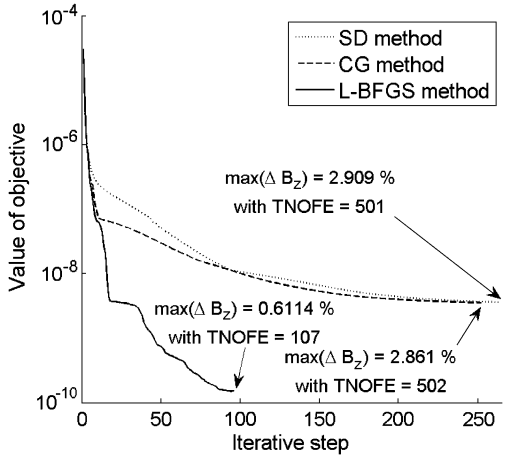

Fig. 8. Convergence comparison among steepest descent, conjugate gradient and L-BFGS methods.

considering the sensitivity expression in (9), the term $\partial B_{zi}/\partial \alpha_j$ requires unchanged in each iteration for the case that the ROI and design surface are spatially fixed, and the discretization mesh of Γ_{coil} and the sampling points of the ROI are kept unchanged. Therefore, one can calculate the elements of the dense

TABLE I
PERFORMANCE OF L-BFGS FOR DIFFERENT VALUES OF M

Value of M in L-BFGS	Iteration loop	Objective evaluation	Residual of objective	Value of $max(\triangle B_z)$
3	194	225	1.3969e-10	0.6485 %
6	153	187	1.4036e-10	0.6040 %
9	95	107	1.5090e-10	0.6114 %
12	86	102	1.5219e-10	0.5744 %
15	91	103	1.4806e-10	0.6079 %
18	67	78	1.6247e-10	0.626 %
21	75	87	1.4861e-10	0.6114 %
24	85	103	1.4790e-10	0.6057 %
27	66	77	1.4965e-10	0.6014 %
30	67	79	1.4908e-10	0.6144 %
33	73	83	1.4834e-10	0.6031 %
36	66	87	1.4874e-10	0.6059 %

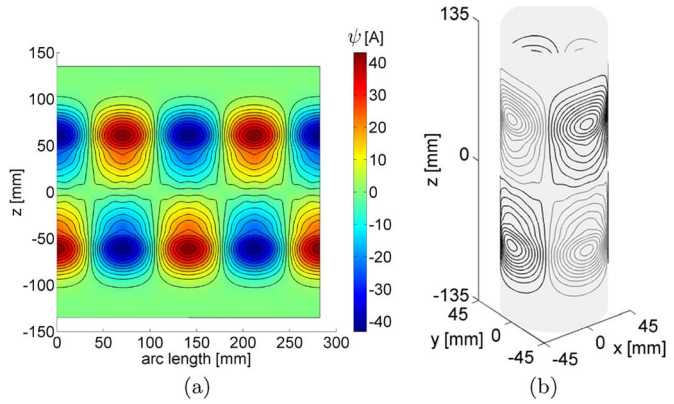

Fig. 9. Stream function contours and its corresponding layout of shim coil for target magnetic field $B_z^* = 0.2(x^2 - y^2)$. (a) Stream function and its contours using L-BFGS with $\mathrm{M} = 9$. (b) Layout of shim coil with current 4.3104A.

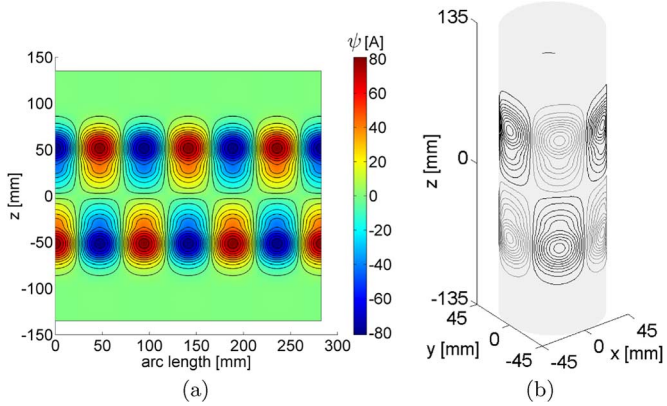

Fig. 10. Stream function contours and its corresponding layout of shim coil for target magnetic field $B_z^* = 10x(x^2 - 3y^2)$. (a) Stream function and its contours using L-BFGS with $\mathrm{M} = 9$. (b) Layout of shim coil with current 8.1035 A.

matrix $\partial B_{zi}/\partial \alpha_j$ once and save them as data. During each iteration, one needs to evaluate the vector $(B_{zi} - B_{zi}^*)$. The sensitivity vector is then the multiplication of the vector $(B_{zi} - B_{zi}^*)$ and the dense matrix $(\partial B_{zi}/\partial \alpha_j)$. If one requires to design other coils, such as different shim coils on the same cylinder domain and ROI, the dense matrix can be re-used for all the original sensitivity analysis. Therefore, the design of MRI coils is a unified procedure in which the user needs to modify the optimization objective in order to design different kinds of coils. The computed optimal shim coil shape with target magnetic fields as

$$B_z^* = 0.2(x^2 - y^2) \tag{18}$$

and

$$B_z^* = 10x(x^2 - 3y^2) \tag{19}$$

are shown in Figs. 9 and 10.

VII. GRADIENT COIL DESIGN BASED ON TWO OBJECTIVES

Except for the target magnetic field distribution, the value of inductance and thermal energy are additional key points to judge the quality of a coil. Therefore, MRI coil design requires multiple objective functions. A number of papers have discussed the design of coils employing an auxiliary objective function, such as the inductance of the coil, the magnetic energy of the coil, or the torque balance of the coil. A variety of methods can deal with multiple objective functions optimization as well [35], [46]. In most cases, one target is chosen as the main objective function and other targets are included into a Lagrangian optimization model by using the augmented Lagrangian method. It is known that the augmented Lagrangian method works well for optimization with equality constraints. Usually designers do not know a realistic value of the inductance, the magnetic energy or the thermal energy, therefore the target magnetic field B_z^* is transformed as an equality constraint and is added into a Lagrangian optimization model using the Lagrange multiplier method. Equation (20) shows a Lagrangian optimization model

$$\text{Min:} \quad F = \int_{\Omega} Obj_1 d\Omega + \int_{\Omega_{\mathrm{ROI}}} \lambda \left(B_z - B_z^*\right) d\Omega_{\mathrm{ROI}} \tag{20}$$

where Obj_1 is the main objective which needs to be minimized, and λ is a Lagrange multiplier used to satisfy the equality constraint $B_z - B_z^* = 0$ inside a ROI. The price one pays for this method is the additional cost to calculate the value of the Lagrange multiplier. Usually, the accuracy of the determined Lagrange multiplier will control the residual of an equality constraint. Therefore, one may meet numerical difficulties when the equality constraint cannot be strictly satisfied. In this paper, the weighted sum objective method is used to design gradient coils and the additional optimization objective function chosen in this paper is the square of the current density which is related with the Joule heating of a coil.

A. Two Objective Optimization

In this section, the Joule heating is added as a second consideration in addition to the target magnetic field distribution. In Joule heating, the temperature increases due to resistive heat dissipation by the electric current $\vec{J}$. The generated resistive heat Q is proportional to the square of the magnitude of the electric current density. Based on the above analysis, the optimization objective functions used here are

$$\text{Min}: F = \omega_1 \int_{\Omega_{\text{ROI}}} (B_z - B_z^*)^2 d\Omega_{\text{ROI}} + \omega_2 \int_{\Gamma_{\text{coil}}} \frac{1}{2t\sigma} |\vec{J}|^2 d\Gamma_{\text{coil}} \tag{21}$$

where ω_i is the weight to balance the performance of the two objective functions, t is the thickness of the surface, and σ is the material conductivity of the coil. In this section, parameters is chosen as $t = 3\ \text{mm}$ and $\sigma = 5.998 \times 10^7$, respectively.

B. Pareto Optimality

Ideally, the two objectives in (21) should effectively control the thermal performance and the magnetic field distribution of a MRI coil. One could obtain a list of optimal solutions, called Pareto optimal, by changing the value of weights ω_i. The notion of Pareto optimality was introduced by Pareto in 1896. A Pareto point is defined by a given set of the multiple objectives. The value of the sum of all objectives represents a Pareto point if it is impossible to minimize the value of any single objective without a simultaneous increasing the value of at least one other objective. For a multiple objective functions optimization in which all the objectives need to be minimized, a very popular and straightforward approach is to sum up different objective functions using a convex combination [47]

$$\sum_{i=1}^{n} \omega_i = 1, \quad \omega_i > 0. \tag{22}$$

A common optimization procedure is to perform the above minimization for an even spread of ω_i in order to generate several points in the Pareto front (or Pareto curve for the two objective case). However, it is known that an even distribution of the weight w_i does not produce an even distribution of the Pareto points along the Pareto curve, even if the Pareto curve is convex. In this paper, the upper lower bound approach which is proposed by Marler and Arora in [48] is used to obtain a relatively even distribution of Pareto points. In the last section, the optimal coil layout was obtained by using only one objective. This optimal solution ($\psi = \psi_{opt}$) and initial value ($\psi = 0$) of the stream function provide us the lower and upper bound for the two objectives in (21) respectively

$$\begin{aligned}
F_{1\,\min} &= \int_{\Omega_{\text{ROI}}} (B_z - B_z^*)^2 d\Omega_{\text{ROI}} \Big|_{\psi=\psi_{\text{opt}}} \\
F_{1\,\max} &= \int_{\Omega_{\text{ROI}}} (B_z - B_z^*)^2 d\Omega_{\text{ROI}} \Big|_{\psi=0} \\
F_{2\,\min} &= \int_{\Gamma_{\text{coil}}} \frac{1}{2t\sigma} |\vec{J}|^2 d\Gamma_{\text{coil}} \Big|_{\psi=0} \\
F_{2\,\max} &= \int_{\Gamma_{\text{coil}}} \frac{1}{2t\sigma} |\vec{J}|^2 d\Gamma_{\text{coil}} \Big|_{\psi=\psi_{\text{opt}}}.
\end{aligned} \tag{23}$$

Therefore, the transformed expression of (21) using the upper lower bound approach is

$$\text{Min}: \quad F = \frac{\omega_1 (F_1 - F_{1\,\min})}{F_{1\,\max} - F_{1\,\min}} + \frac{\omega_2 (F_2 - F_{2\,\min})}{F_{2\,\max} - F_{2\,\min}} \tag{24}$$

where

$$\begin{aligned}
F_1 &= \int_{\Omega_{\text{ROI}}} (B_z - B_z^*)^2 d\Omega_{\text{ROI}} \\
F_2 &= \int_{\Gamma_{\text{coil}}} \frac{1}{2t\sigma} |\vec{J}|^2 d\Gamma_{\text{coil}}.
\end{aligned} \tag{25}$$

During the optimization, the sensitivity for the F_1 is calculated based on (9). For the second objective F_2, the numerical discretization method is used to calculate the sensitivity at the sample points on the design surface Γ_{coil}

$$\begin{aligned}
\frac{\partial F_2}{\partial \alpha_j} &= \sum_{i=1}^{nd} P_{ji} \alpha_i \\
P_{ji} &= \int_{\Gamma_{\text{coil}}} \frac{1}{t\sigma} \nabla \times (N_j \cdot \vec{n}) \cdot \nabla \times (N_i \cdot \vec{n}) d\Gamma_{\text{coil}}.
\end{aligned} \tag{26}$$

In the design of gradient coil, the gradient strength can be improved when a coil is placed closer to the object to be imaged. For example, the head gradient coil [49], [50] has been designed to provide higher performance on gradient than the whole body gradient coil. In this section, the optimization method based on Pareto optimality is used to design cylindrical gradient coil that the design surface has four slots on the top and bottom of surface. Fig. 12 shows a meshed design surface. The coil optimization is implemented by using the same setup for the cylindrical gradient coil shown in the last section. The goal of the gradient strength in the center of the ROI is 10 mT/m. Fig. 11 shows a Pareto curve for the optimization model of (24). This Pareto curve provides a list of Pareto optimal solutions where $\omega_2 = [1e-4 : 1e-4 : 9e-4, 1e-3 : 1e-3 : 9e-3, 1e-2 : 1e-2 : 9e-2, 1e-1 : 1e-1 : 9e-1]$. One optimized layout of coils are shown in Figs. 13 and 14 where the $\max(\Delta B_z)$ in the ROI for G_x and G_z are 0.9087% and 0.9799% for the weight

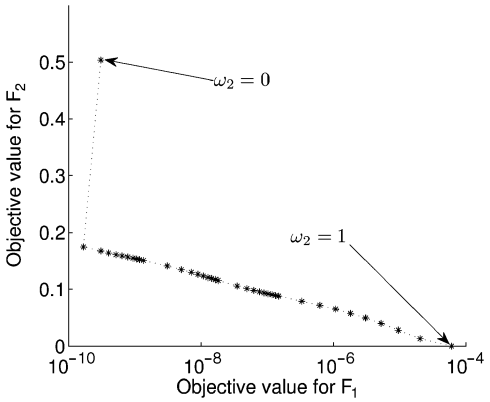

Fig. 11. Pareto curve for the optimization of two-objective functions in equation (21).

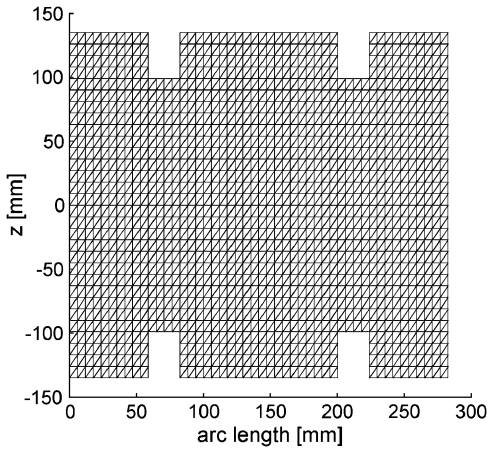

Fig. 12. The mesh on cylindrical developed surface with slots.

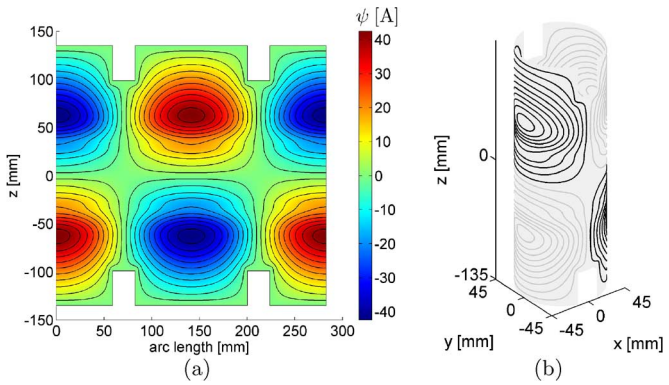

Fig. 13. Stream function contours and its corresponding layout of G_x gradient coil for target magnetic field gradient 10 mT/m. (a) Stream function and its contours using L-BFGS. (b) Layout of G_x gradient coil with current 4.2424A.

$\omega_2 = 0.0004$ and 0.0003 in the Pareto optimality, respectively.

VIII. Conclusion

This paper has shown an efficient iteration optimization method which can be used to design MRI coils on cylindrical surface. A discretization of the stream function with high-order smooth leads to a theoretically continuous expression of the electric current density. During the iterative procedure, there

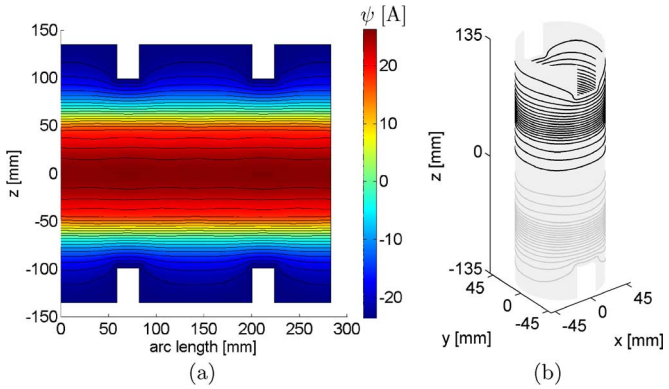

Fig. 14. Stream function contours and its corresponding layout of G_z gradient coil for target magnetic field gradient 10 mT/m. (a) Stream function and its contours using L-BFGS. (b) Layout of G_z gradient coil with current 2.4961A.

is a great deal of flexibility in the optimization technique, including the fast sensitivity analysis, choosing efficient descent direction, smoothing design variables, and limiting the shape of coils. In addition, the Pareto points provide designers more flexible choices in order to balance the performance between two objective functions by using the multiple objective optimization method. This is an alternative optimization methodology when multiple objective functions cannot be combined together by using the Lagrange multipliers.

Acknowledgment

This work was supported by German Federal Ministry of Education and Research (BMBF) INUMAC grant 13N9208, German Research Foundation (DFG) grant 1883/9-1, and the hundred talent project in CAS, China.

References

[1] R. Turner, "A target field approach to optimal coil design," *J. Phys. D*, vol. 19, no. 8, pp. 147–151, Aug. 1986.
[2] R. Turner, "Gradient coil design: A review of methods," *Magn. Reson. Imag.*, vol. 11, no. 7, pp. 903–920, 1993.
[3] P. Mansfield and B. Chapman, "Active magnetic screening of coils for static and time-dependent magnetic field generated in NMR imaging," *J. Phys. E*, vol. 19, no. 7, pp. 540–545, Jul. 1986.
[4] M. Engelsberg, R. E. de Souza, and C. M. D. Pazos, "The limitations of a target field approach to coil design," *J. Phys. D*, vol. 21, no. 7, pp. 1062–1066, Jul. 1988.
[5] R. Turner, "Minimum inductance coils," *J. Phys. E*, vol. 21, no. 10, pp. 948–952, Oct. 1988.
[6] A. M. Abduljalil, A. H. Aletras, and P. M. L. Robitaille, "Torque free asymmetric gradient coils for echo planar imaging," *Magn. Reson. Med.*, vol. 31, no. 4, pp. 450–453, Apr. 1994.
[7] S. Crozier and D. Doddrell, "A design methodology for short, whole body, shielded gradient coils for MRI," *Magn. Reson. Imag.*, vol. 13, no. 4, pp. 615–620, 1995.
[8] D. C. Alsop and T. J. Connick, "Optimization of torque-balanced asymmetric head gradient coils," *Magn. Reson. Med.*, vol. 35, no. 6, pp. 875–886, 1996.
[9] L. K. Forbes and S. Crozier, "A novel target-field method for finite-length magnetic resonance shim coils: I. Zonal shims," *J. Phys. D*, vol. 34, no. 24, pp. 3447–3455, Dec. 2001.
[10] L. Forbes, M. Brideson, and S. Crozier, "A target-field method to design circular biplanar coils for asymmetric shim and gradient fields," *IEEE Trans. Magn.*, vol. 41, no. 6, pp. 2134–2144, Jun. 2005.
[11] S. H. Shvartsman, M. Morich, G. Demeester, and Z. Zhai, "Ultrashort shielded gradient coil design with 3D geometry," *Concepts Magn. Reson.*, vol. 26B, no. 1, pp. 1–5, Aug. 2005.
[12] W. Liu, D. Zu, X. Tang, and H. Guo, "Target-field method for MRI biplanar gradient coil design," *J. Phys. D*, vol. 40, no. 5, pp. 4418–4424, Aug. 2007.

[13] H. Sanchez, F. Liu, A. Trakic, and S. Crozier, "A simple relationship for high efficiency-gradient uniformity tradeoff in multi-layer asymmetric gradient coils for MRI," *IEEE Trans. Magn.*, vol. 43, no. 2, pp. 523–532, Feb. 2007.

[14] L. K. Forbes, M. A. Brideson, S. Crozier, and P. T. While, "An analytical approach to the design of quiet cylindrical asymmetric gradient coils in MRI," *Concepts Magn. Reson.*, vol. 31B, no. 4, pp. 218–236, Oct. 2007.

[15] Y. Zhang, D. Xie, B. Bai, H. S. Yoon, and C. S. Koh, "A novel optimal design method of passive shimming for permanent MRI magnet," *IEEE Trans. Magn.*, vol. 44, no. 6, pp. 1058–1061, Jun. 2008.

[16] P. T. While, L. K. Forbes, and S. Crozier, "3-D gradient coil design—Initial theoretical framework," *IEEE Trans. Biomed. Eng.*, vol. 56, no. 4, pp. 1169–1183, Apr. 2009.

[17] X. Li, D. Xie, and J. Wang, "Design of gradient coil set with canceled net thrust force for fully open MRI system," *IEEE Trans. Magn.*, vol. 45, no. 3, pp. 1804–1807, Mar. 2009.

[18] S. Pissanetzky, "Minimum energy MRI gradient coils of general geometry," *Meas. Sci. Technol.*, vol. 3, no. 7, pp. 667–673, Jul. 1992.

[19] M. A. Brideson, L. K. Forbes, and S. Crozier, "Determining complicated winding patterns for shim coils using stream functions and the target-field method," *Concepts Magn. Reson.*, vol. 14B, no. 1, pp. 9–18, 2002.

[20] G. N. Peeren, "Stream function approach for determining optimal surface currents," *J. Comput. Phys.*, vol. 191, no. 1, pp. 305–321, Oct. 2003.

[21] R. A. Lemdiasov and R. Ludwig, "A stream function method for gradient coil design," *Concepts Magn. Reson.*, vol. 26B, no. 1, pp. 67–80, Aug. 2005.

[22] M. Poole and R. Bowtell, "Novel gradient coils designed using a boundary element method," *Concepts Magn. Reson.*, vol. 31B, no. 3, pp. 162–175, Aug. 2007.

[23] L. Marin, H. Power, R. W. Bowtell, C. C. Sanchez, A. A. Becker, P. Gloverand, and A. Jones, "Boundary element method for an inverse problem in magnetic resonance imaging gradient coils," *CMES-Comp. Model. Eng. Sci.*, vol. 23, no. 3, pp. 149–173, Jan. 2008.

[24] P. W. Gross and P. R. Kotiuga, *Electromagnetic Theory and Computation: A Topological Approach*. Cambridge, U.K.: Cambridge University Press, 2004.

[25] O. C. Zienkiewicz and R. L. Taylor, *The Finite Element Method*, 5th ed. New York: Elsevier, 2000, vol. 1.

[26] P. Daly, "Finite elements for field problems in cylindrical co-coordinates," *Int. J. Numer. Meth. Eng.*, vol. 6, no. 2, pp. 169–178, Jul. 1973.

[27] L. T. Isaacs, "A curved cubic triangular finite element for potential flow problems," *Int. J. Numer. Meth. Eng.*, vol. 7, no. 3, pp. 337–344, Jun. 1971.

[28] D. Zorin, P. Schroeder, and W. Sweldens, "Interpolating subdivision for meshes with arbitrary topology," in *SIGGRAPH Conf. Proc.*, 1996, pp. 189–192.

[29] M. P. do Carmo, *Differential Geometry of Curves and Surfaces*. Upper Saddle River, NJ: Pearson Education, 1976.

[30] F. Shi and R. Ludwig, "Magnetic resonance imaging gradient coil design by combining optimization techniques with the finite element method," *IEEE Trans. Magn.*, vol. 34, no. 3, pp. 671–683, May 1998.

[31] S. E. Ungersma, H. Xu, B. A. Chronik, G. C. Scott, A. Macovski, and S. Conolly, "Shim design using a linear programming algorithm," *Magn. Reson. Med.*, vol. 52, no. 3, pp. 619–627, Sep. 2004.

[32] H. S. Lopez, F. Liu, M. Poole, and S. Crozier, "Equivalent magnetization current method applied to the design of gradient coils for magnetic resonance imaging," *IEEE Trans. Magn.*, vol. 45, no. 2, pp. 767–775, Feb. 2009.

[33] J. H. Argyris, I. Fried, and D. M. Scharpf, "The TUBA family of plate elements for the matrix displacement method," *Aerosp. J. Roy. Aerosp. Soc*, vol. 72, no. 692, pp. 701–709, 1968.

[34] O. C. Zienkiewicz and R. L. Taylor, *The Finite Element Method*, 5th. ed. New York: Elsevier, 2000, vol. 2.

[35] J. Nocedal and S. J. Wright, *Numerical Optimization*. New York: Springer, 1998.

[36] D. C. Liu and J. Nocedal, "On the limited memory BFGS method for large scale optimization methods," *Math. Program.*, vol. 45, no. 3, pp. 503–528, Dec. 1989.

[37] P. E. Gill, W. Murray, and M. H. Wright, *Practical Optimization*. New York: Elsevier, 1982.

[38] M. Zhu, L. Xia, F. Liu, and S. Crozier, "Deformation-space method for the design of biplanar transverse gradient coils in open MRI systems," *IEEE Trans. Magn.*, vol. 44, no. 8, pp. 2035–2041, Aug. 2008.

[39] A. N. Tikhonov and V. Y. Arsenin, *Solution to Ill-Posed Problems*. New York: Winston-Wiley, 1977.

[40] H. W. Engl, M. Hanke, and A. Neubauer, *Regularization of Inverse Problems*. New York: Springer, 1996.

[41] P. C. Hansen, "Regularization tools: A matlab package for analysis and solution of discrete ill-posed problems," *Numer. Algorithms*, vol. 6, no. 1, pp. 1–35, Mar. 1994.

[42] G. Shou, L. Xia, F. Liu, M. Zhu, Y. Li, and S. Crozier, "MRI coil design using boundary-element method with regularization technique: A numerical calculation study," *IEEE Trans. Magn.*, vol. 46, no. 4, pp. 1052–1059, Apr. 2010.

[43] O. Sigmund and J. Petersson, "Numerical instabilities in topology optimization: A survey on procedures dealing with checkerboards, mesh-dependencies and local minimal," *Struct. Multidisc. Optim.*, vol. 16, no. 1, pp. 68–75, Aug. 1998.

[44] M. Y. Wang, S. W. Zhou, and H. Ding, "Nonlinear diffusions in topology optimization," *Struct. Multidisc. Optim.*, vol. 28, no. 4, pp. 262–276, Oct. 2004.

[45] [Online]. Available: http://www.comsol.com

[46] D. Xie, X. Sun, B. Bai, and S. Yang, "Multiobjective optimization based on response surface model and its application to engineering shape design," *IEEE Trans. Magn.*, vol. 44, no. 6, pp. 1006–1009, Jun. 2008.

[47] R. T. Marler and J. S. Arora, "Survey of multi-objective optimization methods for engineering," *Struct. Multidisc. Optim.*, vol. 26, no. 6, pp. 369–395, Apr. 2004.

[48] R. T. Marler and J. S. Arora, "Function-transformation methods for multi-objective optimization," *Eng. Optim.*, vol. 37, no. 6, pp. 551–570, Sep. 2005.

[49] D. C. Alsop and T. J. Connick, "Optimization of torque-balanced asymmetric head gradient coils," *Magn. Reson. Med.*, vol. 35, no. 6, pp. 875–886, Jun. 1996.

[50] B. A. Chronik, A. Alejski, and B. K. Rutt, "Design and fabrication of a three-axis edge ROU head and neck gradient coil," *Magn. Reson. Med.*, vol. 44, no. 6, pp. 955–963, Dec. 2000.